



UNIVERSITÀ DI PARMA

ARCHIVIO DELLA RICERCA

University of Parma Research Repository

Variation in benthic metabolism and nitrogen cycling across clam aquaculture sites

This is the peer reviewed version of the following article:

Original

Variation in benthic metabolism and nitrogen cycling across clam aquaculture sites / Murphy, Anna E.; Nizzoli, Daniele; Bartoli, Marco; Smyth, Ashley R.; Castaldelli, Giuseppe; Anderson, Iris C.. - In: MARINE POLLUTION BULLETIN. - ISSN 0025-326X. - 127:(2018), pp. 524-535. [10.1016/j.marpolbul.2017.12.003]

Availability:

This version is available at: 11381/2837984 since: 2021-10-06T16:18:36Z

Publisher:

Elsevier Ltd

Published

DOI:10.1016/j.marpolbul.2017.12.003

Terms of use:

Anyone can freely access the full text of works made available as "Open Access". Works made available

Publisher copyright

note finali coverpage

(Article begins on next page)

1

2 Variation in benthic metabolism and nitrogen cycling across clam aquaculture sites

3

4 Anna E. Murphy^{1a}, Daniele Nizzoli², Marco Bartoli^{2,3}, Ashley R. Smyth⁴, Giuseppe Castaldelli⁵,
5 Iris C. Anderson¹

6

7 ¹Virginia Institute of Marine Science, College of William & Mary, Gloucester Point, VA 23062,
8 USA

9 ²Department of Chemistry, Life Sciences and Environmental Sustainability, University of Parma,
10 Parco Area delle Scienze 11/A, 43124 Parma, Italy

11 ³Klaipeda University, LT-92294 Klaipeda, Lithuania

12 ⁴Soil and Water Sciences Department, Tropical Research and Education Center, University of
13 Florida, Institute of Food and Agricultural Sciences, Homestead, FL

14 ⁵Department of Life Sciences and Biotechnology, Ferrara University, Italy

15

16 ^aCurrent Address: Marine Science Center, Northeastern University, Nahant, MA 01908

17

18 ABSTRACT

19 As bivalve aquaculture expands globally, an understanding of how it alters nitrogen is
20 important to minimize impacts. This study investigated nitrogen cycling associated with clam
21 aquaculture in the Sacca di Goro, Italy (*Ruditapes philippinarum*) and the Eastern Shore, USA
22 (*Mercenaria mercenaria*). Ammonium and dissolved oxygen fluxes were positively correlated
23 with clam biomass; *R. philippinarum* consumed ~6 times more oxygen and excreted ~5 times

24 more NH_4^+ than *M. mercenaria*. There was no direct effect of clams on denitrification or
25 dissimilatory nitrate reduction to ammonium (DNRA); rather, nitrate availability controlled the
26 competition between these microbial pathways. Highest denitrification rates were measured at
27 sites where both water column nitrate and nitrification were elevated due to high densities of a
28 burrowing amphipod (*Corophium* sp.). DNRA exceeded denitrification where water column
29 nitrate was low and nitrification was suppressed in highly reduced sediment, potentially due to
30 low hydrologic flow and high clam densities.

31

32 **KEYWORDS:**

33 Denitrification; DNRA; nitrification; nitrate respiration; clam aquaculture; nitrogen cycling

34

35

36

37

38 *Acknowledgements*

39 We are grateful to the aquaculturists and Consorzio Pescatori Goro for providing access
40 to the clam leases. MIMS analysis was financed by the Emilia-Romagna Region within the POR
41 FESR 2007-2013 Programme. This work was supported by Virginia Sea Grant
42 (NA10OAR4170085, #R/71515W, #R/715168), the NSF GK12 Fellowship (DGE-0840804), the
43 Strategic Environmental Research and Development Program – Defense Coastal/Estuarine
44 Research Program Project SI-1413, and NSF Virginia Coast Reserve LTER Project (DEB
45 0080381, DEB 061014). The authors declare that they have no conflict of interest. This

46 manuscript is contribution No. XXXX from the Virginia Institute of Marine Science, College of
47 William and Mary.

48 INTRODUCTION

49 The presence of bivalve aquaculture in coastal ecosystems has large implications for
50 coastal nitrogen (N) dynamics. As nutrient pollution continues to be problematic in coastal
51 waters worldwide concurrent with the rapid expansion of the bivalve industry (FAO 2014), the
52 influence of bivalve aquaculture on N removal pathways is of increasing interest. Implementing
53 bivalve aquaculture as a means to promote N removal and mitigate coastal eutrophication is a
54 current topic of debate (e.g. Stadmark & Conley 2011, Rose et al. 2012). Effective resource
55 management requires an understanding of the net effect of bivalve cultivation on N cycling, both
56 recycling and removal pathways, and particularly how this changes with different environmental
57 conditions. This study investigates the mechanistic drivers that influence the effects of clam
58 cultivation on benthic N cycling pathways by sampling two clam species that are farmed across a
59 range of environmental conditions.

60 As infaunal organisms, cultivated clams both directly and indirectly affect sediment N
61 cycling rates and benthic metabolism through bioturbation, biodeposition, excretion, and
62 respiration, which subsequently influence microbial metabolic pathways (reviewed in Laverock
63 et al. 2011). Clam bioturbation transports particles and water, including solutes (e.g. O₂, NO₃⁻),
64 through sediments. Through feeding and biodeposition, clams actively deliver organic carbon to
65 the sediments from the water column, fueling microbial decomposition pathways, enhancing
66 microbial respiration and oxygen demand, and thereby substantially changing redox gradients
67 (Aller 1982, Kristensen et al. 1985) and impacting redox sensitive microbial processes such as
68 nitrification and denitrification (Stief 2013). Benthic infauna, including cultivated clams, also

69 excrete dissolved inorganic and organic N, directly increasing benthic N fluxes to the water
70 column and potentially providing substrate (e.g. NH_4^+) for microbial processes such as
71 nitrification and ANAMMOX (Welsh et al. 2015). Bivalves can thus influence both microbial N
72 removal and recycling pathways in coastal sediments.

73 Bivalves may enhance N removal by promoting denitrification, the microbially mediated
74 pathway that reduces nitrate (NO_3^-) to inert N_2 gas. This bivalve-facilitated, denitrification
75 enhancement results both from biodeposition of organic matter to sediment microbial
76 communities (Newell et al. 2002, Kellogg et al. 2013, Smyth et al. 2013) and by provision of
77 habitats for denitrifying microorganisms (Heisterkamp et al., 2010; Welsh et al., 2015). However,
78 some studies have reported no significant effect of bivalves on denitrification rates (Higgins et al.
79 2013, Erler et al. 2017). Additionally, often overlooked is the effect bivalves have on inorganic
80 N regeneration pathways. High densities of bivalves, found in cultivation settings, may
81 accelerate N recycling processes through bivalve excretion and stimulation of microbial
82 ammonification including dissimilatory nitrate reduction to ammonium (NH_4^+) (DNRA) (Dame
83 2011, Murphy et al. 2016, Erler et al. 2017), which retain bioavailable N in the aquatic
84 ecosystem.

85 The question of whether bivalves promote N removal or retention remains equivocal.
86 The discrepancy among previous studies on how bivalves influence benthic N cycling pathways
87 is in part due to differences in the bivalve species studied (e.g. epifaunal oysters or mussels
88 versus infaunal clams), but also likely due differences in the environmental conditions under
89 which bivalves are farmed. Bivalve aquaculture can occupy expansive regions across estuarine
90 environmental gradients. Few studies that investigate N cycling associated with bivalve
91 aquaculture, and specifically clam aquaculture, have captured the natural environmental

92 variability across which the practice exists. Moreover, few studies have investigated the
93 partitioning of NO_3^- reduction between denitrification and DNRA, which is ecologically
94 important as DNRA retains bioavailable N in the system as NH_4^+ whereas denitrification
95 removes it. Those studies that do provide simultaneous measurements of denitrification and
96 DNRA are restricted to single study systems. Therefore, we were interested in directly
97 comparing different study systems, which are heavily exploited for infaunal clam cultivation and
98 where previous studies found contrasting results regarding denitrification and DNRA at clam
99 cultivation sites. We chose to sample clam aquaculture in the Sacca di Goro, Italy, where
100 denitrification was reportedly higher than DNRA (Nizzoli et al. 2006) and in coastal Virginia,
101 US, where DNRA generally dominated NO_3^- respiration (Murphy et al. 2016).

102 The objective of this study was to investigate how sediment N cycling associated with
103 clam aquaculture varies across different environmental conditions and between two commonly
104 cultivated infaunal clam species: *Ruditapes philipinarum* (Italy) and *Mercenaria mercenaria*
105 (US). Across the natural environmental gradients in which clam aquaculture exists, we were
106 specifically interested in (1) comparing N cycling and metabolic rates between the two cultivated
107 clam species and determining the direct contribution of these clams to benthic rates and (2)
108 determining the factors that influence the competition between microbial denitrification and
109 DNRA at clam aquaculture sites. By studying two clam species exposed to different
110 environmental conditions and farming practices, we sought to highlight the challenge in
111 generalizing ecological responses across all bivalve aquaculture and, more specifically, across all
112 clam cultivation practices. We hypothesized that both clam species would significantly increase
113 benthic oxygen demand and inorganic N fluxes; however, the contribution of clams to these
114 benthic processes would differ across sites depending on site-specific factors and clam species

115 physiology. We expected that the degree to which N is removed through denitrification relative
116 to N recycled through DNRA would change depending on the availability of labile organic
117 carbon and NO_3^- (Tiedje 1988), factors that would vary broadly across estuarine gradients and
118 clam aquaculture sites.

119

120 METHODS

121 *Study Sites*

122 The Sacca di Goro is a lagoonal system of the Po River Delta, Italy. Approximately 26
123 km^2 with an average depth of 1.5 m, the lagoon hosts a substantial clam aquaculture industry,
124 with about 1/3 of the area occupied by clam cultivation. The system is generally divided into
125 three areas based on hydrologic characteristics: the eastern portion is shallow with low energy
126 and slow water exchange; the central region is tidally influenced, and the western portion is
127 riverine dominated with freshwater flow from the Po di Volano (Figure 1A). The lagoon,
128 particularly the eastern region, typically experiences periodic dystrophic events in the early
129 summer when macroalgae bloom. Drastic changes to the hydrodynamics of the system were
130 made over the past 20 years to improve water flow and alleviate dystrophic events, including
131 channel construction along the southern sand spit and dredging of internal canals to increase flow
132 to the Adriatic Sea (Viaroli et al. 2006). The manila clam, *R. philippinarum*, is farmed in
133 privately leased portions of the lagoon at densities ranging from 100 to >2000 individuals m^{-2} .
134 Growers collect juvenile clams at the mouth and directly outside the lagoon, transport them to
135 individual leases within the lagoon; after approximately 9 months market-sized clams are
136 hydraulically harvested.

137 Clam aquaculture occupies large subtidal areas on both the Chesapeake Bay-side and
138 Atlantic-side of the Eastern Shore peninsula of Virginia (Emery 2015). Cherrystone Inlet (ES-
139 23), located on the Chesapeake Bay-side of the Eastern Shore, is a small shallow embayment (~6
140 km², mean water depth of 1.1 m) that receives little freshwater discharge. Smith Island Bay (ES-
141 33) is the southern-most lagoon, located on the eastern side of the Eastern Shore and is protected
142 from the Atlantic Ocean by a barrier island (Figure 1B). In both locations, the hard clam, *M.*
143 *mercenaria*, is cultivated in privately owned leases in subtidal regions. Clams are sourced from
144 land-based hatcheries and nurseries and planted in the sediments at ~8-15 mm in shell length.
145 Unlike in Italy, growers set plastic mesh nets over the clam beds flush to the sediment surface as
146 protection from natural predation. Macroalgal blooms, supported by nutrients excreted by clams
147 and from microbial mineralization of organic matter in the sediment, occur on the predator-
148 exclusion nets (Murphy et al. 2015). Periodically growers sweep the nets of macroalgae to
149 prevent the algae from suffocating the clams. After about two years the market-sized clams are
150 hydraulically harvested.

151

152 *Site Characterization*

153 Surface water column and sediment samples were collected once in summer 2013 at five
154 sites in the Sacca di Goro, Italy (Figure 1A) and two sites on the Eastern Shore, VA USA (Figure
155 1B). Triplicate water column grab samples were collected at each site at ~50 cm above the
156 sediment, filtered (0.45 µm) and stored frozen in either whirlpak bags or Falcon tubes until
157 analyzed for NH₄⁺ and nitrate plus nitrite (NO_x⁻). Triplicate sediment cores (polycarbonate core
158 tubes, 30 cm height and 4 cm i.d.) were also collected at each site for determination of sediment
159 organic matter by loss on ignition (450 °C over 3 hours) in the 0-2 cm sediment horizon.

160 Temperature and salinity were measured at each site using a thermometer and refractometer,
161 respectively. Although, both the Sacca di Goro and the Eastern Shore experience seasonal
162 variation in temperature, salinity, and nutrient concentrations (Murphy et al. 2016; Nizzoli et al.
163 2006), capturing this temporal variability was beyond the scope of this study. We focused on the
164 natural spatial variability of environmental parameters across the study sites during the summer
165 season, when biogeochemical rates are typically high. Throughout the study, site identification
166 refers to the location and measured salinity, for example, Goro-13 was collected in the Sacca di
167 Goro and the salinity was 13.

168

169 *Benthic Metabolism and Nutrient Flux Measurements – ‘Intact Cores’*

170 Twelve sediment cores (10 cm sediment depth) were collected (Eastern Shore (ES) sites,
171 9.5cm i.d.; Goro sites, 8 cm i.d.) at all sites, except ES-23 where 10 cores were collected, for the
172 determination of benthic metabolism, nutrient fluxes, denitrification and DNRA. From each site,
173 half the cores were incubated in the light and half in the dark. Cores were randomly collected at
174 each site; clam densities varied between sediment cores and some sediment cores contained no
175 clams by chance.

176 Sediment cores collected in the Sacca di Goro were transported to the University of
177 Parma while cores from the Eastern Shore were transported to Virginia Institute of Marine
178 Science, Eastern Shore Laboratory (VIMS ESL) in Wachapreague VA. Cores were placed in
179 water baths at site-specific salinity and temperature and allowed to equilibrate overnight. Oxic
180 conditions in water baths were assured by bubbling with airstones. The water inside the cores
181 was gently stirred avoiding sediment resuspension during the equilibration and incubation
182 periods with magnetic stirrers driven by a large magnet rotated by an external motor at 40 rpm.

183 The following day, half the cores were illuminated while the other half remained dark. The water
184 inside the tanks was replaced with new water prior to initiating the incubation. To initiate
185 incubations, the water level in the tank was lowered to below the core tops and all cores were
186 sealed with clear lids. Short term batch incubations were conducted over 4-5 hours, ensuring
187 cores never became hypoxic or anoxic. At each time point, DO was measured and samples of
188 overlying water were collected for determinations of NH_4^+ and NO_x^- . Water column nutrient
189 samples were immediately filtered (0.45 μm) and stored frozen until analysis. For the Sacca di
190 Goro incubations, a polarographic microsensor (50 μm ; Unisense, DK) connected to an
191 amperometer (PA2000, Unisense, DK) was used to measure DO concentrations in water samples
192 collected during the incubation, stored in 12 ml exetainers (Labco Inc.) and preserved with ZnCl_2
193 (100 μl of 7M solution). For the Eastern Shore sites, DO was measured using Hach LDO101
194 Luminescent dissolved oxygen (DO) sensors (Hach Co., Loveland, CO, USA) secured in the lids
195 of the cores. Hourly fluxes for each analyte ($\text{mmol O}_2 \text{ m}^{-2} \text{ hr}^{-1}$ or $\mu\text{mol N m}^{-2} \text{ hr}^{-1}$) were
196 calculated as the change in concentration over time multiplied by the core water volume and
197 divided by the core surface area. Fluxes from the sediment to the water column are represented
198 by positive values (production), while fluxes to the sediment from the water column are negative
199 (consumption).

200

201 *Denitrification and DNRA Rate Measurements – ‘Intact Cores’*

202 After the initial flux incubations for NH_4^+ , NO_x^- , and DO, all cores were uncapped and
203 the overlying water was replaced. Cores were allowed to equilibrate in the water bath for at least
204 one hour; the light cores remained illuminated and the dark cores remained dark. The isotope
205 pairing technique (IPT) was used to measure denitrification (Nielsen 1992) and DNRA

206 (Risgaard-Petersen & Rysgaard 1995). The water bath level was dropped to just below the core
207 tops; $^{15}\text{NO}_3^-$ (98.9 atom %, targeting a final concentration of $\sim 100 \mu\text{M}$) was added to the
208 overlying water of each core. A water sample was collected from each core immediately before
209 and after $^{15}\text{NO}_3^-$ addition to determine the ^{15}N -enrichment of the NO_3^- pool. Then the cores were
210 capped and sealed. Incubations typically lasted 3-4 hours, depending on the specific sediment
211 oxygen demand determined in the previous incubation (see above), allowing DO to change by no
212 more than 30% of the initial concentration (Dalsgaard et al. 2000). After the incubation, each
213 core was gently homogenized and slurries were sampled for $^{29}\text{N}_2$, $^{30}\text{N}_2$, and extractable $^{15}\text{NH}_4^+$.

214 Dissolved $^{29}\text{N}_2$ and $^{30}\text{N}_2$ gas samples were collected by siphoning the homogenized core
215 slurry into 12 ml exetainer vials (Labco, Inc) without headspace and preserving them with 100 μl
216 of ZnCl_2 (7M). The abundances of $^{29}\text{N}_2$ and $^{30}\text{N}_2$ in the dissolved N_2 pool were determined
217 within a month on a membrane inlet mass spectrometer (MIMS, detection limits for $^{29}\text{N}_2$ and
218 $^{30}\text{N}_2$ are 0.011 and 0.0004 μM , respectively) (Kana et al. 1994) using a PrismaPlus mass
219 spectrometer with an inline furnace operated at 600 $^\circ\text{C}$ to allow for O_2 removal (limits of
220 detection for $^{29}\text{N}_2$ and $^{30}\text{N}_2$ are 10 nM and 0.4 nM, respectively). Denitrification rates were
221 calculated based on the production of $^{29}\text{N}_2$ (p29) and $^{30}\text{N}_2$ (p30), assuming a binomial
222 distribution of $^{28}\text{N}_2$, $^{29}\text{N}_2$, and $^{30}\text{N}_2$ (Nielsen 1992) as follows:

223

$$224 \quad D_{15} = p_{29} + 2p_{30} \quad (3)$$

225

$$226 \quad D_{14} = D_{15} \times (p_{29}/2p_{30}) \quad (4)$$

227

228 where D_{15} represents denitrification of the added $^{15}\text{NO}_3^-$ and D_{14} is the ambient denitrification
229 rate of $^{14}\text{NO}_3^-$. Direct denitrification of NO_3^- from the water column (D_w) and coupled
230 denitrification (D_n) were calculated as described by Nielsen (1992):

231

$$232 \quad D_w = (^{14}\text{NO}_3^- / ^{15}\text{NO}_3^-) * D_{15} \quad (5)$$

233

$$234 \quad D_n = D_{14} - D_w \quad (6)$$

235

236 where $^{14}\text{NO}_3^-$ is equal to the ambient unlabeled NO_3^- concentration (μM) and $^{15}\text{NO}_3^-$ is equal to
237 the isotopically-labeled NO_3^- concentration at the start of the incubation. Previous manipulation
238 experiments in which denitrification rates were measured with various concentrations of added
239 $^{15}\text{NO}_3^-$, demonstrated that at all sites ANAMMOX contributed a negligible amount of N_2 relative
240 to denitrification (Murphy, unpublished). Thus, the assumptions upon which the isotope pairing
241 technique is based were met and the equations are valid for these systems (Nielsen 1992).

242 The homogenized cores were also sampled for extractable $^{15}\text{NH}_4^+$ to calculate ambient
243 DNRA rates from the production of $^{15}\text{NH}_4$. Potassium chloride (KCl) was added to
244 approximately 200 ml of sediment slurry for a final concentration of 2M. Samples were shaken
245 for 1 hour, filtered (0.45 μm Whatman PES), and frozen until they were diffused and trapped for
246 analyses of $^{15}\text{NH}_4^+$ enrichment and concentration using a method modified from Brooks (1989).
247 Water samples were placed in specimen cups; an acidified (25 μl of 2.5M sulfuric acid) GFF
248 filter (1cm, i.d.), threaded onto a stainless steel wire, was suspended on the lip of the cup;
249 magnesium oxide was added and the samples were allowed to diffuse for 2 weeks, after which

250 samples were placed in tin capsules and analyzed on an isotope ratio mass spectrometer (IRMS)
251 at the University of California Davis Stable Isotope Facility for $^{15}\text{NH}_4^+$.

252 DNRA rates of the ambient $^{14}\text{NO}_3^-$ (DNRA_t) were calculated according to Risgaard-
253 Petersen & Rysgaard (1995) as:

254

$$255 \quad \text{DNRA}_t = p^{15}\text{NH}_4^+ \times (\text{D}_{14}/\text{D}_{15}) \quad (7)$$

256

257 where $p^{15}\text{NH}_4^+$ is equal to the production of $^{15}\text{NH}_4^+$. This assumes that DNRA occurs in the same
258 sediment horizon as denitrification, resulting in the same proportional use of $^{14}\text{NO}_3^-$ and $^{15}\text{NO}_3^-$
259 as denitrification (Rysgaard et al. 1993). Direct DNRA of NO_3^- from the water column
260 (DNRA_w) and coupled DNRA (DNRA_n) were calculated as:

261

$$262 \quad \text{DNRA}_w = (^{14}\text{NO}_3^- / ^{15}\text{NO}_3^-) * p^{15}\text{NH}_4^+ \quad (8)$$

263

$$264 \quad \text{DNRA}_n = \text{DNRA}_t - \text{DNRA}_w \quad (9)$$

265

266 Nitrification rates were estimated as the sum of denitrification, DNRA, and NO_x^- effluxes.

267

268 *Clam Respiration and Excretion Rate Measurements – ‘Clam-Only Incubations’*

269 After the ‘intact sediment core’ incubations, all sediment cores were sieved and the clams
270 from each core were collected and rinsed to remove any sediment; these clams were placed back
271 into the same polycarbonate tubes they were sieved from for a ‘clam-only’ (i.e. no sediment)
272 incubation. Therefore, the number of clams in each tube varied across samples and reflected the

273 ambient clam density at each study site. ‘Clam-only’ static flux incubations were then conducted
274 as described for the ‘intact sediment core’ incubations. Chambers with the clams were placed
275 back in the water bath, filled with unfiltered water, allowed to equilibrate for at least an hour, and
276 capped for 2-3 hours. Over the incubation, samples were collected for DO, NH_4^+ and NO_3^- . As
277 described above, hourly fluxes for each analyte ($\text{mmol O}_2 \text{ m}^{-2} \text{ hr}^{-1}$ or $\mu \text{ mol N m}^{-2} \text{ hr}^{-1}$) were
278 calculated as the change in concentration over time multiplied by the core water volume and
279 divided by the core surface area. All these incubations were conducted under dark conditions.
280 After the incubations, all clams were measured (shell length) and tissue dry weight (DW) and
281 ash-free DW (loss on ignition) were obtained.

282

283 *Infauna Sampling*

284 After initial observations during field sampling, it was determined that a burrowing
285 amphipod, *Corophium* sp., was present at Goro-10, Goro-13, and Goro-15. As these organisms
286 likely strongly influence N cycling rates (Steif et al. 2013), we collected, counted, and
287 determined biomass (g DW m^{-2}) of the amphipods. As this decision was made after sampling
288 Goro-10 and Goro-16, amphipod data were not collected at these sites, although it was clear that
289 amphipods were also abundant at Goro-10. Amphipods were not abundant at the Eastern Shore
290 sites and were not quantified (pers. obs.).

291

292 *Gross Microbial Ammonification Rates*

293 Additional core samples were collected at each site for gross ammonification rate
294 measurements using the isotope pool dilution technique (Anderson et al. 1997). Cores (5.7 cm
295 i.d, with approximately 5 cm overlying water and 5 cm sediment depth) were collected in pairs at

296 each sampling site, carefully avoiding inclusion of clams, however other infauna were retained.
 297 It is important to note that this method cannot decipher between microbial and infaunal NH_4^+
 298 production; it is not possible to remove infaunal organisms without disturbing the natural
 299 sediment gradients important to microbial metabolic pathways. Cores were transported to the
 300 laboratory, placed in site water, and held overnight uncapped with gentle mixing and aeration.
 301 The following day the sediments were uniformly spiked with $^{15}\text{N-NH}_4^+$ (3.6 ml of $[\text{NH}_4]_2\text{SO}_4$, 30
 302 at.%, 10 mM). One paired core, T_0 , was immediately sacrificed after spiking by shaking in 2M
 303 KCl for an hour; the extractant was filtered and frozen until analysis. The T_f cores were capped
 304 and incubated for 24 hours in the dark at *in situ* temperatures, after which the cores were
 305 processed the same as the T_0 cores above. NH_4^+ was processed and analyzed using the diffusion
 306 method modified by Brooks 1989, as described above. Rates of gross ammonification were
 307 calculated using a model described by Wessel & Tietema 1992 as

308
 309

$$\begin{aligned}
 & \text{Ammonification} = \frac{\ln(T_{f_{\text{atm}\%}} - k) / (T_{0_{\text{atm}\%}} - k)}{\ln[\text{NH}_4^+ T_f] / [\text{NH}_4^+ T_0]} * \frac{[\text{NH}_4^+ T_0] - [\text{NH}_4^+ T_f]}{\text{time}} \\
 & (10)
 \end{aligned}$$

313
 314

315 where $T_{f_{\text{atm}\%}}$ and $T_{0_{\text{atm}\%}}$ refer to the $^{15}\text{NH}_4^+$ enrichment of the T_f and T_0 cores; k is equal to
 316 natural abundance of $^{15}\text{NH}_4^+$ expressed as atom %; $[\text{NH}_4^+ T_f]$ and $[\text{NH}_4^+ T_0]$ are the concentrations
 317 of NH_4^+ in the T_f and T_0 cores, respectively, and time is the incubation time.

318

319 *Denitrification Efficiency Calculation*

320 Denitrification efficiency, the percent of organic N that is mineralized via denitrification,
321 was calculated as:

322

323 Denitrification Efficiency (%) = $\frac{D_{14}}{NO_x^- + NH_4^+ + D_{14}} \times 100$ (11)

324

325 where D_{14} is denitrification and NO_x^- and NH_4^+ represent the positive fluxes of these nutrients
326 (effluxes).

327

328 *Statistical Analyses*

329 Data from the ‘clam-only’ incubations were analyzed using analysis of covariance
330 (ANCOVA) to test the effect of and interaction between clam biomass and species on rate
331 measurements (NH_4^+ , NO_x^- , and DO fluxes). Clam physiological rates (respiration and excretion),
332 were calculated using the slope estimates of the linear models within each species ($mmol O_2 g$
333 $DW^{-1} hr^{-1}$ or $\mu mol NH_4^+ g DW^{-1} hr^{-1}$). To determine the clam contribution to total benthic fluxes,
334 clam physiological rates were scaled to per m^2 by multiplying by the clam biomass present
335 within each core and dividing by the surface area of the core and compared to the ‘intact core’.

336 A two-way analysis of variance (ANOVA) was used to examine the interactive effects of
337 light condition and site, which refers to all 7 study sites, on ‘intact sediment’ nutrient fluxes, DO
338 fluxes, denitrification, and DNRA. Tukey HSD post hoc analysis was used to compare means
339 when an effect was significant. For further analysis, all fluxes, regardless of whether they were
340 made in the light or dark were included and the effect of light was ignored because (1) the
341 ANOVAs revealed light condition had minimal effects on the response variables and (2) the

342 effect of light on benthic biogeochemical rates was not a priority of our study, however we
343 included paired light and dark cores to capture the variability associated with light in our
344 measurements.

345 Linear models were used to assess the relationship between clam biomass and ‘intact core’
346 rate measurements (nutrient and DO fluxes, denitrification, and DNRA) within each site
347 individually. Across all sites, the overall effects of clam biomass and species on ‘intact sediment’
348 nutrient fluxes, DO fluxes, denitrification, and DNRA, were assessed using mixed effects models,
349 which accounted for the variance due to site. The mixed effects models (*lme* function from the
350 ‘nlme’ package (Pinheiro et al. 2017)) were constructed with clam biomass and species as fixed
351 effects while site was included as a random effect. Both the intercept and slope were allowed to
352 vary by site to account for intrinsic site differences that may affect baseline benthic rates as well
353 as differences in clam behavior or metabolisms across the sites.

354 Linear models were used to examine the effect of *Corophium* abundances on rates of
355 denitrification, DNRA, and estimated nitrification across the three sites in which *Corophium*
356 were quantified. Finally, the ratio of DNRA to denitrification (DNRA : DNF) as a function of
357 labile organic carbon (ammonification rates were considered a proxy) relative to NO_3^-
358 availability (ammonification rate : water column NO_3^-) was explored with a linear model.

359 Data were checked for normality and homogeneity of variance using the Shapiro-Wilk
360 and Levene’s tests and transformed using Box-Cox to meet assumptions. All statistical analyses
361 were considered significant at the $p < 0.05$ level and were conducted in R Studio, version 3.4.1.

362

363 RESULTS

364 *Environmental Characteristics*

365 Salinity ranged from 10 to 33, while temperature was relatively consistent with lower
366 temperatures at the Sacca di Goro sites (20-21 °C) than the Eastern Shore sites (25-27°C) (Table
367 1). Water column NO_x^- was inversely correlated with salinity ($R^2 = 0.74$, $p = 0.01$), with the
368 highest concentration at Goro-10 (54 μM) and lowest concentration at ES-23 (0.2 μM). Water
369 column NH_4^+ ranged from 0.88 μM at ES-33 to 38.4 μM at Goro-16, with no significant
370 relationship with salinity. Sediment organic matter (0-2 cm sediment horizon) was highest at
371 Goro-15 (2.38) and lowest at Goro-16 (0.92), but was generally similar across sites.

372 Average clam densities in the Sacca di Goro ranged from 365 to 2089 individuals m^{-2} ,
373 and increased with salinity in this system ($R^2 = 0.88$, $p = 0.01$), while average densities on the
374 Eastern Shore ranged from 258 to 630 individuals m^{-2} and did not follow the salinity trend (Table
375 2). Average clam biomass ranged from 82.9 to 553 g DW m^{-2} and was not significantly related to
376 salinity (Table 2). *M. Mercenaria* were generally larger, averaging 39.7 mm in shell length,
377 compared to the *R. philippinarum*, which ranged from 24.5 to 32.5 mm.

378 *Corophium* densities ranged from an average of 534 ind m^{-2} at Goro-21 to 20,783 ind m^{-2}
379 at Goro-13 (Table 2). Based on visual estimation during sampling the densities at Goro-10 were
380 similar to densities measured at the nearby sites (Goro-13 and Goro-15); however, densities were
381 not directly quantified.

382

383 *Dissolved Oxygen Fluxes*

384 The 'clam only' incubations revealed significantly different respiration rates between the
385 two species (ANCOVA, $p < 0.001$); *R. philippinarum* had significantly higher rates of
386 respiration ($0.024 \pm 0.002 \text{ mmol O}_2 \text{ g DW}^{-1} \text{ hr}^{-1}$) compared to *M. mercenaria*, which averaged

387 $0.006 \pm 0.001 \text{ mmol O}_2 \text{ g DW}^{-1} \text{ hr}^{-1}$ (Table 3). Clam respiration accounted for between 18 and
388 176% of the ‘intact sediment’ dark DO fluxes across sites.

389 The ‘intact sediment’ incubations revealed all sites to be net heterotrophic (DO
390 consuming) and ranged from a mean of $-3.0 \pm 0.6 \text{ mmol m}^{-2} \text{ hr}^{-1}$ in the light at ES-23 to a mean
391 of $-21.8 \pm 3.2 \text{ mmol m}^{-2} \text{ hr}^{-1}$ in the light at Goro-15 (Figure 2A). There was no significant effect
392 of light on DO fluxes; a significant site effect was observed, with highest consumption at Goro-
393 13 and Goro-15 (Supplemental Table 1, Figure 2A). Within each site individually, ‘intact
394 sediment’ DO fluxes were significantly correlated with clam biomass, except at Goro-10 and ES-
395 23 (Supplemental Table 2). Across all sites, there was a significant effect of clam biomass on
396 ‘intact sediment’ DO fluxes, while the effect of clam species was not significant (Figure 3A,
397 Table 4).

398

399 *NH₄⁺ Fluxes*

400 Similar to clam respiration, the clam excretion rates, measured in the ‘clam only’
401 incubations, were significantly higher for *R. philippinarum*, averaging $2.73 \pm 0.27 \text{ } \mu\text{mol N g}$
402 $\text{DW}^{-1} \text{ hr}^{-1}$, compared to *M. mercenaria*, which averaged $0.75 \pm 0.10 \text{ } \mu\text{mol N g DW}^{-1} \text{ hr}^{-1}$
403 (ANCOVA, $p < 0.001$, Table 3). Clam excretion accounted for between 28 and 575% of the total
404 benthic NH_4^+ fluxes.

405 There was no significant effect of light or site on the ‘intact sediment’ NH_4^+ fluxes
406 (Supplemental Table 1). All sites had a net efflux of NH_4^+ in the light and dark, ranging from an
407 average of 101.6 ± 42.7 to $1258.7 \pm 173.5 \text{ } \mu\text{mol m}^{-2} \text{ hr}^{-1}$ at Goro-10 and Goro15, respectively.
408 (Figure 2B). Within each site individually, ‘intact sediment’ NH_4^+ fluxes were significantly
409 positively correlated with clam biomass, except at Goro-15, ES-23, and ES-33 (Supplemental

410 Table 2). Across all sites, net NH_4^+ fluxes were significantly positively correlated with clam
411 biomass, while the effect of clam species was not significant (Figure 3B, Table 4).

412

413 *NO_x⁻ Fluxes*

414 In the ‘clam only’ incubations NO_x^- fluxes were not significantly related to clam biomass
415 for either species (ANCOVA, $p = 0.97$). In the ‘intact sediment’ incubations NO_x^- fluxes were
416 negligible at the high salinity sites (ES-33, ES-23, and Goro-21). Sediments were a net sink of
417 NO_x^- at the mid-salinity site (Goro-16), averaging $-250.0 \pm 73.6 \mu\text{mol m}^{-2} \text{hr}^{-1}$, and shifted to a
418 net source of NO_x^- to the water column at the low salinity sites (Goro-10 and Goro-13), which
419 averaged $1349.2 \pm 238.3 \mu\text{mol m}^{-2} \text{hr}^{-1}$ and $606.2 \pm 120.0 \mu\text{mol m}^{-2} \text{hr}^{-1}$, respectively (Figure 2C).

420 A significant interaction was observed between site and light condition, driven mainly by the
421 significantly higher NO_x^- efflux in the dark at Goro-10 (Figure 2C, Supplemental Table 1).

422 There was no significant relationship between ‘intact sediment’ NO_x^- fluxes and clam biomass
423 (mixed effect model, $p = 0.41$, Table 4). Within each site individually, ‘intact sediment’ NO_x^-
424 fluxes were not related to clam biomass, except at ES-33, where the relationship was
425 significantly negative (Supplemental Table 2). NO_x^- fluxes across the sites were significantly
426 inversely related to salinity ($R^2 = 0.21$, $p < 0.001$) and directly related to water column NO_3^-
427 concentrations ($R^2 = 0.23$, $p < 0.001$).

428

429 *Gross Ammonification Rates*

430 Gross microbial ammonification rates were significantly lower at ES-23, averaging $2.4 \pm$
431 $0.3 \text{ mmol m}^{-2} \text{d}^{-1}$, compared to the other sites (Table 5). The high salinity sites in the Sacca di

432 Goro (Goro-16 and Goro-21) had rates similar to ES-23 and were significantly lower than the
433 up-estuary sites (Goro-15 and Goro-13), which averaged $11.5 \text{ mmol m}^{-2} \text{ d}^{-1}$ (Table 5).

434

435 *Denitrification, DNRA, and Nitrification*

436 Average denitrification rates ranged from $1.6 \pm 0.2 \text{ } \mu\text{mol m}^{-2} \text{ hr}^{-1}$ at ES-23 to $259.1 \pm$
437 $54.1 \text{ } \mu\text{mol m}^{-2} \text{ hr}^{-1}$ at Goro-10. There was no significant effect of light on denitrification rates,
438 however rates were significantly different across sites (Supplemental Table 1). ES-23, ES-33,
439 and Goro-21 had similar denitrification rates, which were significantly lower than the other sites
440 (Figure 4A). Overall nitrification was the main nitrate source for denitrification at ES-23, ES-33,
441 and Goro-21, where D_n ranged from 78 to 98% of D_{14} (Table 5). Despite the high water column
442 NO_x^- concentrations at the low salinity sites (Goro-10, Goro-13, and Goro-15), the percent of
443 denitrification coupled to nitrification was $>50\%$, suggesting high nitrification rates (Table 5).
444 At Goro-16, where water column NO_x^- was high ($\sim 30 \text{ } \mu\text{M}$), the percent denitrification coupled to
445 nitrification was only 27% (Figure 4A, Table 5). Within each site individually, there was no
446 effect of clam biomass on denitrification except at Goro-13, where denitrification increased with
447 clam biomass (Supplemental Table 2). Across all sites, there was no significant effect of clam
448 biomass or species on denitrification rates (Table 4). Denitrification efficiency was generally
449 low at all sites, ranging from 6.6% in ES-23 to 30.5% at Goro-15 (Table 5).

450 DNRA rates ranged from $8.2 \pm 1.2 \text{ } \mu\text{mol m}^{-2} \text{ hr}^{-1}$ at Goro-13 to $87.7 \pm 22.5 \text{ } \mu\text{mol m}^{-2} \text{ hr}^{-1}$
451 at Goro-16 (Figure 4B). There was no significant effect of light on DNRA rates (Supplemental
452 Table 1). DNRA was significantly higher at Goro-16 compared to all other sites (Figure 4B;
453 Supplemental Table 1). In general, there was no significant effect of clam biomass or species on
454 total DNRA (Table 4). However when considered within each site, total DNRA significantly

455 increased with clam biomass at Goro-10 and Goro-13, while clam biomass had no significant
456 effect on DNRA at any of the other sites (Supplemental Table 2).

457 Across sites in which *Corophium* sp. abundances were quantified (i.e. Goro-13, Goro-15,
458 and Goro-21), DNRA rates were significantly negatively correlated with *Corophium* sp.
459 abundances (Figure 5A), while rates of denitrification and calculated nitrification were
460 significantly positively correlated with *Corophium* sp. abundances (Figure 5B and 5C).
461 However, these relationships should be considered with caution as the environmental variability
462 across the three sites may be confounding and could not be fully assessed statistically with the
463 limited number of sites in which *Corophium* sp. were quantified (e.g. using a mixed effects
464 model).

465 The ratio of DNRA relative to denitrification (DNRA : DNF) was highest at ES-33,
466 averaging 14.9, and lowest at Goro-13, averaging 0.06 (Table 5). Denitrification exceeded
467 DNRA at Goro-10, Goro-15, Goro-13, while DNRA exceeded denitrification at Goro-21, ES-23,
468 and ES-33; at Goro-16 DNRA : DNF was close to 1. The means of DNRA : DNF across sites
469 were positively correlated with the ratio of ammonification (a proxy for labile carbon
470 availability) relative to water column NO_x^- concentration ($p < 0.001$) (Figure 6).

471

472 DISCUSSION

473 This study demonstrates the importance of considering environmental factors,
474 specifically those influencing NO_3^- supply, when determining the effects of clam cultivation on
475 N removal and recycling processes. By sampling across clam aquaculture sites that spanned two
476 countries and a range of environmental conditions, this study captured some of the natural
477 environmental variability under which clam aquaculture is practiced. However, as this study was

478 field-based with randomly selected sites, there was little control over environmental conditions.
479 Strong negative covariance between water column NO_3^- concentrations and salinity made it
480 difficult to determine the mechanistic controls on the observed differences in rates across
481 sampling sites. Despite this, the data provide insight into the influence of bivalve aquaculture on
482 sediment biogeochemistry and specifically N processing. The study shows the effects of bivalves
483 depends on the local environment and the specific bivalve species cultivated. As such, the
484 ecosystem impact of clam aquaculture should be assessed accordingly.

485

486 *Clam bioenergetics directly affect NH_4^+ and DO fluxes*

487 Our results highlight the difference in metabolic rates between the two infaunal clam
488 species. *R. philippinarum* consumed approximately 6 times more oxygen and regenerated
489 approximately 5 times more NH_4^+ than *M. mercenaria*. These differences could be due to
490 intrinsic species-specific physiological and/or behavioral differences, size/age differences, and/or
491 variation in food sources between the regions. The fact that *R. philippinarum* has higher
492 metabolism may suggest that this species also has higher filtration rates than *M. mercenaria*.
493 Depending on food availability, which varies by location, *R. philippinarum* may deliver more
494 organic carbon to the sediments than *M. mercenaria*. The methods used to estimate clam
495 respiration and excretion in this study assume that clams behave similarly when removed from
496 the sediment as they do *in situ*. However, our rates reflect reasonable approximations, as they
497 are similar to previously reported rates for *M. mercenaria* (Srna & Baggaley 1976, Hofmann et
498 al. 2006) and *R. philippinarum* (Magni & Montani 2005, Han et al. 2008) measured at similar
499 temperatures.

500 The relative importance of clam metabolism to total benthic community respiration and
501 NH_4^+ production varied across sites depending on clam biomass present. However, clam
502 biomass only explained 30% and 37% of the variation in DO and NH_4^+ fluxes, respectively
503 (marginal R^2 of mixed effect models, Figure 3). This indicates that other processes are likely
504 important in dictating DO and NH_4^+ , such as microbial metabolism and the metabolism of other
505 dominant infauna present. Clam respiration accounted for a high percentage of dark DO
506 consumption at the down-estuary sites in the Sacca di Goro (68-176%) where clam biomass was
507 high, concurrent with low ammonification rates and low sediment organic matter relative to the
508 other sites, suggesting lower microbial respiration. By contrast, clam respiration accounted for
509 <50% of total dark DO consumption where high abundances of the burrowing amphipod
510 *Corophium* sp. were present ($\sim 20,000$ ind m^{-2}) (Goro-10, Goro-13, and Goro-15). *Corophium*
511 sp. not only contribute directly to benthic community respiration but, through bioirrigation, may
512 stimulate oxygen-consuming microbial pathways such as nitrification and aerobic decomposition
513 (Steif 2013; Figure 5). Finally, despite the high clam biomass present at the US sites, clam
514 respiration accounted for <20% of the benthic DO consumption. These sediments have been
515 reported as being highly reduced with high pore water sulfide concentrations (Murphy et al.
516 2016; Smyth et al. *in review*); therefore, microbial respiration and the re-oxidation of reduced
517 compounds such as sulfide may consume the majority of oxygen at these sites.

518

519 *Locally, clams have little effect on denitrification, DNRA, and NO_x^- fluxes*

520 Previous studies have shown that by depositing organic matter to the sediment surface
521 and by providing substrate for bacteria to colonize (i.e. clam microbiome), clams increase nitrate
522 respiration rates (e.g. Nizzoli et al. 2006, Kellogg et al. 2013, Welsh et al. 2015). However, in

523 this study, within each of the seven study sites, clam biomass had little to no direct effect on
524 denitrification, DNRA, or net NO_x^- fluxes as demonstrated by the linear model analyses of these
525 rates as a function of clam biomass within each site individually (Supplemental Table 2). When
526 the relationship was significant, the effect was small, generally an order of magnitude lower than
527 the effect of clams on NH_4^+ and DO fluxes. This suggests that on a local scale, other factors
528 aside from labile clam biodeposits (assuming clam biomass is related to biodeposition) are
529 important in regulating NO_3^- reduction pathways. For example, as discussed below, factors that
530 strongly influence NO_3^- supply (e.g. burrowing *Corophium*) may be more important in
531 controlling N-cycling rates.

532 There was no effect of clam biomass on denitrification or NO_x^- flux, which is in contrast
533 to a previous study conducted in the winter in the central portion of the Sacca di Goro; a positive
534 relationship between denitrification and NO_x^- consumption with *R. philippinarum* biomass was
535 reported (Welsh et al. 2015). Differences in sampling locations within the Sacca di Goro and
536 season (i.e. water column NO_x^- concentrations and temperature) likely contribute to the
537 conflicting findings. Based on incubations of isolated clams with water column NO_3^-
538 approximately 70 μM , Welsh et al. (2015) concluded that nitrifying and denitrifying
539 microorganisms are harbored within the clam tissue and thus, clams directly exert strong controls
540 on benthic N cycling processes. It is possible that our study did not indicate a major control of
541 clams on these processes during the summer because other factors that affect organic carbon and
542 NO_3^- availability (e.g. salinity, bioturbation, and sulfide) are more important than the clams
543 themselves in regulating NO_3^- respiration pathways, as discussed in more detail below. For
544 example, at the sites where water column NO_3^- was high, the presence of *Corophium* sp. and

545 their strong influence on denitrification may have masked the relationship between clams and
546 denitrification.

547

548 *Spatial variability of denitrification and DNRA is likely driven by NO_3^- and C supply*

549 The mixed effect models which tested the overall effect of clam biomass on rates of
550 denitrification and DNRA while controlling for the variance across sites, showed no significant
551 effect of clam biomass on denitrification or DNRA (Table 4). We expected clam biodeposition to
552 directly provide organic carbon for heterotrophic denitrification and DNRA. It is possible that
553 clam biomass was not the best predictor to capture clam influences on these microbial pathways.
554 Alternatively or in addition, other environmental factors may be driving organic carbon and
555 nitrate dynamics aside from the clams across these heterogenous sites.

556 Assuming ammonification is a reasonable proxy for the lability of organic carbon, the
557 ratio of ammonification to water column NO_3^- , was an important predictor for the partitioning of
558 NO_3^- between DNRA and denitrification across study sites (Figure 6). At sites with a high labile
559 carbon to NO_3^- ratio, DNRA dominated (i.e. the Eastern Shore sites and eastern region of the
560 Sacca di Goro). Denitrification outcompeted DNRA at sites with lower labile carbon to NO_3^-
561 ratios (i.e. low salinity sites in the Sacca di Goro). These trends corroborate previous studies that
562 show strong mechanistic controls of labile carbon relative to NO_3^- on the competition among
563 these two pathways (Hardison et al. 2015, Algar and Vallino 2014). In this study, NO_3^- supply to
564 the sediments and factors that influence this supply strongly affected the competition between
565 DNRA and denitrification across the study sites.

566 When NO_3^- was readily available either from the water column or nitrification,
567 denitrification was favored over DNRA. This is likely due to the fact that denitrification is a

568 more energetically favorable pathway than DNRA (Tiedje 1988; Hardison et al. 2015). This
569 occurred in the western portion of the Sacca di Goro (Goro-10, Goro-13, and Goro-15) where not
570 only was water column NO_3^- high ($\sim 60 \mu\text{M}$) but nitrification rates and NO_3^- effluxes were also
571 high (Table 5; Figure 2C; Figure 4). Approximately 50-65% of denitrification was coupled to
572 nitrification at these sites despite the ample NO_3^- in the water column, indicating high sediment
573 nitrification rates. Elevated nitrification may be associated with the high abundances of the
574 amphipod *Corophium* sp. found at these sites ($\sim 4,800$ - $35,600$ individual m^{-2}). These amphipods
575 can stimulate nitrification (Figure 5C) by creating extensive oxic niches associated with their
576 shallow 'U'-shaped burrows and increasing exchanges of porewater through the sediment profile
577 and overlying water (Henriksen et al. 1983, Middelburg et al. 1996, Kristensen 2000).

578 Additionally, as this study and previous studies have shown, denitrification is enhanced in
579 sediments with high densities of *Corophium* sp., likely due to a tight coupling between
580 nitrification and denitrification within the burrow walls (Pelegri et al. 1994; Figure 5B).

581 At sites where NO_3^- was limiting due to a combination of low ambient water column
582 NO_3^- concentrations, low nitrification rates, and possibly competition with benthic microalgae for
583 NO_3^- (although not directly measured), DNRA dominated NO_3^- respiration (i.e ES-23, ES-33,
584 and Goro-21). Since water column NO_3^- concentrations were low at these sites both
585 denitrification and DNRA were tightly coupled to nitrification (~ 78 - 98%) (Table 5). However,
586 low oxygen availability likely suppressed nitrification at these sites. The generally reduced state
587 of the sediments at the US sites was evidenced by a net release of NH_4^+ and high sediment
588 oxygen consumption with clam metabolism only accounting for approximately 25% of these
589 rates. Additionally, the US sites and the eastern region of the Sacca di Goro were reported as
590 having high sulfide concentrations (Murphy et al. 2016, Giordani et al. 1997), which may

591 directly inhibit nitrification (Joye & Hollibaugh 1995). The use of predator exclusion nets at the
592 US sites, which become fouled by macroalgae (Murphy et al. 2015), likely leads to reduced
593 conditions limiting water flow and exchange between the sediments and water column (Secrist
594 2013). Similarly, in the shallow, sheltered, eastern region of the Sacca di Goro, where the
595 hydrological residence time is long, significant macroalgal blooms occur seasonally and have
596 been associated with large dystrophic events (as reviewed in Viaroli et al. 2006).

597 Highest rates of DNRA occurred in the central portion of the Sacca di Goro (Goro-16),
598 where denitrification rates were also relatively high and the ratio between the two pathways was
599 close to one. Strong competition for NO_3^- between these two NO_3^- respiring pathways was likely
600 due to high water column NO_3^- concurrent with high densities of clams that continuously deliver
601 labile carbon to the sediments. This results in rapid utilization of NO_3^- , as demonstrated by the
602 net influx of NO_3^- (Figure 2C), and a balance between denitrification and DNRA.

603

604 Denitrification efficiency

605 Denitrification efficiency is a metric often used to assess the percent of organic N that is
606 microbially mineralized via denitrification and related to organic carbon load to the benthos
607 (Eyre and Ferguson 2009). However, it also includes any N ‘mineralized’ by infauna (i.e.
608 excretion). In this study, the sediments associated with clam cultivation had low denitrification
609 efficiency (<30%; Table 5). This was not necessarily because denitrification was an unimportant
610 mineralization pathway, in fact it was important in the up-estuary Sacca di Goro sites, but rather
611 because of the high NH_4^+ production by the clams and other infauna. Additionally, bioturbating
612 infauna such as *Corophium* sp., which stimulate denitrification also promote nitrification (Figure
613 5). As observed at the low salinity sites in the Sacca di Goro (Goro-10, Goro-13, and Goro-15),

614 NO_3^- production can exceed consumption, likely due to the *Corophium* sp. flushing their burrows,
615 actively transporting NO_3^- to the water column. This results in high NO_3^- effluxes and
616 subsequently low denitrification efficiencies.

617

618 Conclusions

619 This study demonstrates the variability in N cycling processes in sediments dominated by
620 clam aquaculture. The growth of the clam aquaculture industry in coastal systems worldwide
621 has increased interest in the influence of these operations on coastal N dynamics and specifically
622 the question of whether N removal is promoted through bivalve-facilitated denitrification. This
623 study shows that numerous factors affecting sources of labile carbon, NO_3^- , and O_2 including
624 clam biomass, the presence of other dominant infauna, cultivation practices, and the
625 environmental context determine whether bivalve cultivation favors N loss (i.e. denitrification)
626 or N recycling (i.e. DNRA). Our study further highlights the challenge in generalizing about the
627 influence of clam aquaculture on denitrification and the importance of considering
628 environmental factors and competing pathways (i.e. DNRA). A commonality that was apparent
629 across all study sites was that clams promoted high N recycling and NH_4^+ release to the water
630 column, due to high excretion rates; thus, determination of whether clam aquaculture promotes
631 denitrification or not should be considered within the context of its influence on N regeneration.

632

633 *Literature Cited.*

634

635 Algar CK, Vallino JJ (2014) Predicting microbial nitrate reduction pathways in coastal sediments.

636 *Aquat Microb Ecol* 71:223–238

637 Aller RC (1982) The Effects of Macrobenthos on Chemical Properties of Marine Sediment and

638 Overlying Water. In: *Animal-sediment relations*. Springer US, Boston, MA, p 53–102

639 Anderson IC, Tobias CR, Neikirk BB, Wetzel RL (1997) Development of a process-based

640 nitrogen mass balance model for a Virginia (USA). *Mar Ecol Prog Ser* 159:13–27

641 Bernhard AE, Tucker J, Giblin AE, Stahl DA (2007) Functionally distinct communities of

642 ammonia-oxidizing bacteria along an estuarine salinity gradient. *Environ Microbiol* 9:1439–

643 1447

644 Burgin AJ, Hamilton SK (2007) Have we overemphasized the role of denitrification in aquatic

645 ecosystems? A review of nitrate removal pathways. *Frontiers in Ecology and the*

646 *Environment* 5:89–96

647 Dalsgaard T, Nielsen LP, Brotas V, Viaroli P (2000) Protocol handbook for NICE-Nitrogen

648 Cycling in Estuaries: a project under the EU research programme: *Marine Science and*

649 *Technology (MAST III)*.

650 Erler, D.V., Welsh, D.T., Bennet, W.W., Meziane, T., Hubas, C., Nizzoli, D., Ferguson, A.J.P. The

651 impact of suspended oyster farming on nitrogen cycling and nitrous oxide production in

652 a sub-tropical Australian estuary (2017) *Estuarine, Coastal and Shelf Science*, 192: 117-

653 127.

654

655 FAO (2014) The State of World Fisheries and Aquaculture. Food and Agriculture Organization
656 of the United Nations:1–243

657 Giblin A, Tobias C, Song B, Weston N, Banta G, Rivera-Monroy V (2013) The Importance of
658 Dissimilatory Nitrate Reduction to Ammonium (DNRA) in the Nitrogen Cycle of Coastal
659 Ecosystems. *oceanog* 26:124–131

660 Giordani G, Azzoni R, Bartoli M, Viaroli P (1997) Seasonal variations of sulphate reduction
661 rates, sulphur pools and iron availability in the sediment of a dystrophic lagoon (Sacca di
662 Goro, Italy). *Water, Air and Soil Pollution*, 99 (1-4): 363-371

663 Han KN, Lee SW, Wang SY (2008) The effect of temperature on the energy budget of the
664 Manila clam, *Ruditapes philippinarum*. *Aquacult Int* 16:143–152

665 Hardison AK, Algar CK, Giblin AE, Rich JJ (2015) Influence of organic carbon and nitrate
666 loading on partitioning between dissimilatory nitrate reduction to ammonium (DNRA) and N.
667 *Geochimica et Cosmochimica Acta* 164:146–160

668 Henriksen K, Rasmussen MB, Jensen A (1983) Effect of bioturbation on microbial nitrogen
669 transformations in the sediment and fluxes of ammonium and nitrate to the overlaying water.
670 *Ecological Bulletins*:193–205

671 Hofmann EE, Klinck JM, Kraeuter JN, Powell EN, Grizzle RE, Buckner SC, Bricelj VM (2006)
672 A population dynamics model of the hard clam, *Mercenaria mercenaria*: development of the
673 age-and length-frequency structure of the population. *Journal of Shellfish Research* 25(2):
674 417-444

- 675 Joye SB, Hollibaugh JT (1995) Influence of sulfide inhibition of nitrification on nitrogen
676 regeneration in sediments. *Science* 270:623–625
- 677 Kana TM, Darkangelo C, Hunt MD, Oldham JB, Bennett GE, Cornwell JC (1994) Membrane
678 inlet mass spectrometer for rapid high-precision determination of N₂, O₂, and Ar in
679 environmental water samples. *Analytical Chemistry* 66:4166–4170
- 680 Kellogg ML, Cornwell JC, Owens MS (2013) Denitrification and nutrient assimilation on a
681 restored oyster reef. *Mar Ecol Prog Ser* 480:1–19
- 682 Kristensen E (2000) Organic matter diagenesis at the oxic/anoxic interface in coastal marine
683 sediments, with emphasis on the role of burrowing animals. *Hydrobiologia* 426:1–24
- 684 Kristensen E, Jensen MH, Andersen TK (1985) The impact of polychaete (*Nereis virens* Sars)
685 burrows on nitrification and nitrate reduction in estuarine sediments. *Journal of Experimental*
686 *Marine Biology and Ecology* 85:75-91.
- 687 Laverock B, Gilbert JA, Tait K, Osborn AM, Widdicombe S (2011) Bioturbation: impact on the
688 marine nitrogen cycle. *Biochm Soc Trans* 39:315–320
- 689 Magni P, Montani S (2005) Laboratory experiments on bivalve excretion rates of nutrients. In:
690 Lehr, J, Keeley, J, Lehr, J, and Kingery, TB (eds) *Water Encyclopedia*. John Wiley & Sons,
691 Inc. pp 1-5
- 692 Megonigal JP, Hines ME, Visscher PT (2004) Anaerobic Metabolism: Linkages to trace gases
693 and aerobic processes. In: Schlesinger WH (ed) *Elsevier-Pergamon*, pp 317–424
- 694 Middelburg JJ, Klaver G, Nieuwenhuize J, Wielemaker A, de Haas W, Vlug T, van der Nat

695 JFWA (1996) Organic matter mineralization in intertidal sediments along an estuarine
696 gradient. *Mar Ecol Prog Ser* 132:157-168

697 Murphy AE, Anderson IC, Luckenbach MW (2015) Enhanced nutrient regeneration at
698 commercial hard clam (*Mercenaria mercenaria*) beds and the role of macroalgae. *Mar Ecol*
699 *Prog Ser* 530:135–151

700 Murphy AE, Anderson IC, Smyth AR, Luckenbach MW, and Song B (2016) Dissimilatory
701 nitrate reduction to ammonium (DNRA) exceeds denitrification in hard clam cultivation
702 sediments. *Limnology and Oceanography* DOI 10.1002/lno.10305.

703 Newell RI, Cornwell JC, Owens MS (2002) Influence of simulated bivalve biodeposition and
704 microphytobenthos on sediment nitrogen dynamics: A laboratory study. *Limnol Oceanogr*
705 47:1367–1379

706 Nielsen LP (1992) Denitrification in sediment determined from nitrogen isotope pairing. *FEMS*
707 *Microbiology Letters* 86:357–362

708 Nizzoli D, Welsh DT, Fano EA, Viaroli P (2006) Impact of clam and mussel farming on benthic
709 metabolism and nitrogen cycling, with emphasis on nitrate reduction pathways. *Mar Ecol*
710 *Prog Ser* 315:151–165

711 Pelegri SP, Nielsen LP, Blackburn TH (1994) Denitrification in estuarine sediment stimulated by
712 the irrigation activity of the amphipod *Corophium volutator*. *Mar Ecol Prog Ser* 105:285–
713 290

714 Pinheiro J, Bates D, DebRoy S, Sarkar D and R Core Team (2017). *nlme: Linear and nonlinear*

715 mixed effects models. R package version 3.1-131, [https://CRAN.R-](https://CRAN.R-project.org/package=nlme)
716 [project.org/package=nlme](https://CRAN.R-project.org/package=nlme)

717 Risgaard-Petersen N, Rysgaard S (1995) Nitrate reduction in sediments and waterlogged soil
718 measured by 15N techniques. In: Methods in applied soil microbiology. Academic Press,
719 London, p 1–13

720 Rose JM, Ferreira JG, Stephenson K, Bricker SB, Tedesco M, Wikfors GH (2012) Comment on
721 Stadmark and Conley (2011) "Mussel farming as a nutrient reduction measure in the Baltic
722 Sea: Consideration of nutrient biogeochemical cycles" Marine Pollution Bulletin 64:449–
723 451

724 Rysgaard S, Risgaard-Petersen N, Nielsen LP, Revsbech NP (1993) Nitrification and
725 Denitrification in Lake and Estuarine Sediments Measured by the 15N Dilution Technique
726 and Isotope Pairing. Applied and Environmental Microbiology 59:2093–2098

727 Rysgaard S, Thastum P, Dalsgaard T (1999) Effects of salinity on NH₄⁺ adsorption capacity,
728 nitrification, and denitrification in Danish estuarine sediments. Estuaries 22(1):21-30

729 Seitzinger S, Harrison JA, Böhlke JK, Bouwman AF, Lowrance R, Peterson B, Tobias C, Van
730 Drecht G (2006) Denitrification across landscapes and waterscapes: a synthesis. Ecological
731 Applications 16:2064–2090

732 Seitzinger SP (1988) Denitrification in freshwater and coastal marine ecosystems: ecological and
733 geochemical significance. Limnol Oceanogr 33(4, part 2):702-724

734 Smyth AR, Geraldini NR, Piehler MF (2013) Oyster-mediated benthic-pelagic coupling modifies

735 nitrogen pools and processes. *Mar Ecol Prog Ser* 493:23–30

736 Srna RF, Baggaley A (1976) Rate of excretion of ammonia by the hard clam *Mercenaria*
737 *mercenaria* and the American oyster *Crassostrea virginica*. *Mar Biol* 36:251–258

738 Stadmark J, Conley DJ (2011) Mussel farming as a nutrient reduction measure in the Baltic Sea:
739 Consideration of nutrient biogeochemical cycles. *Marine Pollution Bulletin* 62:1385–1388

740 Stief P (2013) Stimulation of microbial nitrogen cycling in aquatic ecosystems by benthic
741 macrofauna: mechanisms and environmental implications. *Biogeosciences* 10:7829–7846

742 Tiedje JM (1988) Ecology of denitrification and dissimilatory nitrate reduction to ammonium.
743 In: Zehnder A (Ed.) *Biology of anaerobic microorganisms*:179–244

744 Viaroli P, Giordani G, Bartoli M, Naldi M, Azzoni R, Nizzoli D, Ferrari I, Comenges JMZ,
745 Bencivelli S, Castaldelli G, Fano EA (2006) The Sacca di Goro Lagoon and an Arm of the
746 Po River. In: *The Handbook of Environmental Chemistry*. Springer-Verlag,
747 Berlin/Heidelberg, p 197–232

748 Welsh DT, Nizzoli D, Fano EA, Viaroli P (2015) Direct contribution of clams (*Ruditapes*
749 *philippinarum*) to benthic fluxes, nitrification, denitrification and nitrous oxide emission in a
750 farmed sediment. *Estuarine, Coastal and Shelf Science* 154:84–93

751 Wessel WW, Tietema A (1992) Calculating gross N transformation rates of ¹⁵N pool dilution
752 experiments with acid forest litter: analytical and numerical approaches. *Soil Biology and*
753 *Biochemistry* 24:931–942

Figure Captions

Fig 1 Study sites in the Sacca di Goro, Italy (a) and the Eastern Shore, VA, USA (b)

Fig 2 Intact sediment fluxes of dissolved oxygen (a), NH_4^+ (b), and NO_x^- (c), in the light (white) and dark (gray). Letters designate significant differences due to site (DO fluxes; panel a) or the significant interaction of site and light condition (NO_x^- fluxes; panel c). No significant difference due to site or light condition was observed for the NH_4^+ fluxes (b). Sites are organized by salinity. Error bars are standard errors. Inset in (c) shows Goro-21, Cherrystone Inlet (ES-23) and Smith Island (ES-33) on a smaller scale

Fig 3 ‘Intact sediment’ fluxes of dissolved oxygen (a) and NH_4^+ (b) as a function of clam biomass (g DW m^{-2}) at each site from the intact sediment incubations. Data were analyzed using mixed effects models with site as a random effect. The black dashed line represents the fixed effects (clam biomass) while the colored lines show the random effect coefficients for each site. Statistical results are provided in Table 4.

Fig 4 Denitrification (DNF) (a) and DNRA rates (b), in the light (white) and dark (gray), including the portion coupled to nitrification, D_n and DNRA_n (dotted) and direct (NO_x^- from the water column), D_w and DNRA_w (solid). No significant effect of light condition was observed for either parameter. Letters indicate significant differences across sites. Error bars are standard errors. Inset in (a) shows Goro-21, Cherrystone Inlet (ES-23) and Smith Island (ES-33) on smaller scale

Fig 5 Relationship between *Corophium* sp. abundance and DNRA (a), denitrification (b), estimated nitrification (calculated as the sum of denitrification, DNRA, and NO_x^- efflux) (c) at Goro-13 (triangles), Goro-15 (squares), and Goro-21 (circles)

Fig 6 The competition between DNRA and denitrification ($\text{DNRA} : D_{14}$) as a function of the ratio of labile carbon (estimated as ammonification rate (AMN) to water column NO_x^-). Dashed line represents the linear model.

Table 1. Environmental characteristics at each site. Mean values and (standard error).

Site	Salinity	Temp. (°C)	NO _x ⁻ (μM)	NH ₄ ⁺ (μM)	Sediment Organic Matter (0-2cm)
Goro-10	10	20	53.98 (3.43)	19.11 (1.45)	1.36 (0.06)
Goro-13	13	21	33.96 (1.13)	8.50 (0.41)	1.74 (0.05)
Goro-15	15	21	40.04 (0.66)	9.51 (0.36)	2.38 (0.35)
Goro-16	16	20	34.84 (0.59)	38.4 (2.32)	0.92 (0.08)
Goro-21	21	20	1.07 (0.03)	18.43 (1.06)	1.62 (0.09)
ES-23	23	25	0.20 (0.02)	2.10 (0.55)	1.21 (0.11)
ES-33	33	27	0.25 (0.03)	0.88 (0.27)	1.50 (0.15)

Table 2. Clam and *Corophium* sp. data. Mean values and (standard error). n.d., no data collected.

Site	Clam density (ind m ⁻²)	Clam biomass (g DW m ⁻²)	Clam shell length (mm)	<i>Corophium</i> sp. density (ind m ⁻²)	<i>Corophium</i> sp. biomass (g DW m ⁻²)
Goro-10	398 (139)	82.9 (31.7)	28.0 (0.79)	n.d.*	n.d.*
Goro-13	365 (117)	87.1 (26.0)	28.0 (1.03)	20,783 (2,307)	5.46 (0.60)
Goro-15	1161 (268)	188.9 (40.6)	25.8 (0.44)	19,550 (2,581)	7.10 (1.20)
Goro-16	1127 (193)	553.0 (103.4)	32.5 (0.64)	n.d.	n.d.
Goro-21	2089 (478)	316.9 (64.4)	24.5 (0.35)	533 (154)	0.36 (0.10)
ES-23	630 (102)	192.4 (27.8)	35.5 (1.81)	n.d.	n.d.
ES-33	258 (95)	192.4 (84.9)	43.9 (2.02)	n.d.	n.d.

* High abundances of *Corophium* sp. were observed at Goro-10, comparable to the nearby Goro-13 and Goro-15 (pers. obs.).

Table 3

Response	Source of Variation	Estimate	Standard Error	t value	p value	R ²	F Stat	p value	Residual SE	Metabolic Rate
NH ₄ ⁺	Intercept	-198.3	148.1	-1.34	0.18	0.69	F _(3,88) = 68.9	<0.001	455.4	Excretion (μmol gDW ⁻¹ hr ⁻¹)
	Clam biomass	0.75	0.35	2.14	0.04					<i>M. mercenaria</i> : 0.75
	Species	279.89	168.3	1.66	0.10					<i>R. philippinarum</i> : 2.73
	Clam x Species	1.98	0.41	4.8	<0.001					
DO	Intercept	-1.65	1.01	-1.64	0.11	0.80	F _(3,85) = 115.1	<0.001	2.92	Respiration (mmol gDW ⁻¹ hr ⁻¹)
	Clam biomass	-0.006	0.002	-2.62	0.02					<i>M. mercenaria</i> : 0.006
	Species	-0.77	1.13	-0.68	0.50					<i>R. philippinarum</i> : 0.026
	Clam x Species	-0.02	0.003	-6.36	<0.001					
NO _x ⁻	Intercept	4.35	398.6	0.011	0.99	0.11	F _(3,87) = 4.81	0.003	1205	
	Clam biomass	-0.028	0.98	-	0.98					
	Species	-1082	451.3	-2.30	0.02					
	Clam x Species	1.71	1.14	1.50	0.14					

Table 3. ANCOVA results of the ‘clam only’ incubation data. A significant interaction term suggests significant differences in metabolic rates between the two clam species. Figure 3 depicts DO and NH₄⁺ mixed models graphically.

Table 4

Response	Predictor	Estimate	Standard Error	p value	Marginal R ²	Conditional R ²
NH ₄ ⁺	Clam Biomass	2.36	0.81	0.005	0.37	0.7
	Species	293.2	227.1	0.25		
DO	Clam Biomass	-0.01	0.001	<0.001	0.3	0.61
	Species	5.65	3.47	0.16		
NO _x ⁻	Clam Biomass	-0.14	0.16	0.41	0.06	0.66
	Species	-349.1	462.8	0.48		
D ₁₄	Clam Biomass	2.3E-03	0.03	0.94	0.01	0.44
	Species	-135.5	70.7	0.12		
DNRA	Clam Biomass	0.01	0.01	0.42	0.02	0.44
	Species	-9.19	23.3	0.711		

Table 4. Statistical results of the mixed effects models that accounted for the variance associated with site as random, allowing both the intercept and slope to vary: lme(response ~ clam biomass + Species, random = ~Clam Biomass|Site). Interactive effects between clam biomass and species were not significant for any response variable and thus were removed from the models.

Table 5. Average measured gross ammonification rates, calculated nitrification (the sum of D_n , $DNRA_n$, and NO_x^- flux), percent of denitrification coupled to nitrification (% D_n), denitrification efficiency (DNF efficiency), relative proportion of DNRA to denitrification (DNRA:DNF), and ammonification rates relative to water column NO_x^- concentrations (AMN : NO_x^-) at each site. n.d. no data collected.

Site	Ammonification ($mmol\ m^{-2}\ d^{-1}$)	Calculated Nitrification ($\mu mol\ m^{-2}\ hr^{-1}$)	Percent coupled DNF (%)	DNF Efficiency (%)	DNRA : DNF	AMN : NO_x^-
Goro-10	8.06 (0.98)	1656.9 (249.2)	51.4 (7.1)	18.0 (4.3)	0.11 (0.02)	0.14 (0.01)
Goro-13	11.47 (1.6)	762.5 (112.4)	64.5 (1.5)	25.3 (10.3)	0.06 (0.01)	0.25 (0.03)
Goro-15	11.64 (2.6)	405.9 (76.0)	60.2 (1.9)	30.5 (8.2)	0.11 (0.01)	0.24 (0.04)
Goro-16	4.81 (0.79)	185.6 (29.4)	27.4 (8.7)	12.8 (3.3)	1.53 (0.70)	0.15 (0.02)
Goro-21	4.71 (1.17)	58.1 (6.2)	78.2 (2.3)	11.7 (5.8)	2.27 (0.40)	3.18 (0.50)
ES-23	2.38 (0.29)	53.9 (11.8)	93.0 (1.2)	6.6 (3.8)	9.73 (2.30)	11.96 (1.40)
ES-33	n.d.	46.4 (14.0)	97.9 (0.1)	20.5 (11.9)	14.94 (6.10)	n.d.

Figure 1

[Click here to download high resolution image](#)

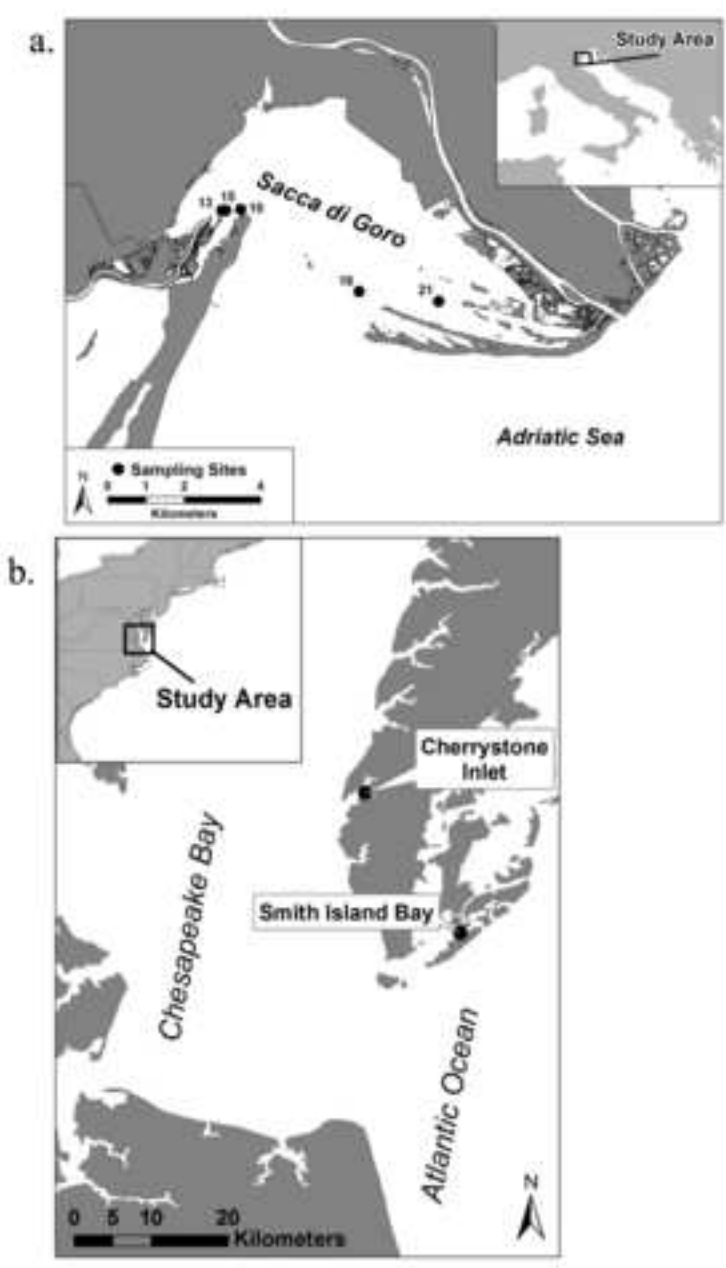


Figure 2

[Click here to download high resolution image](#)

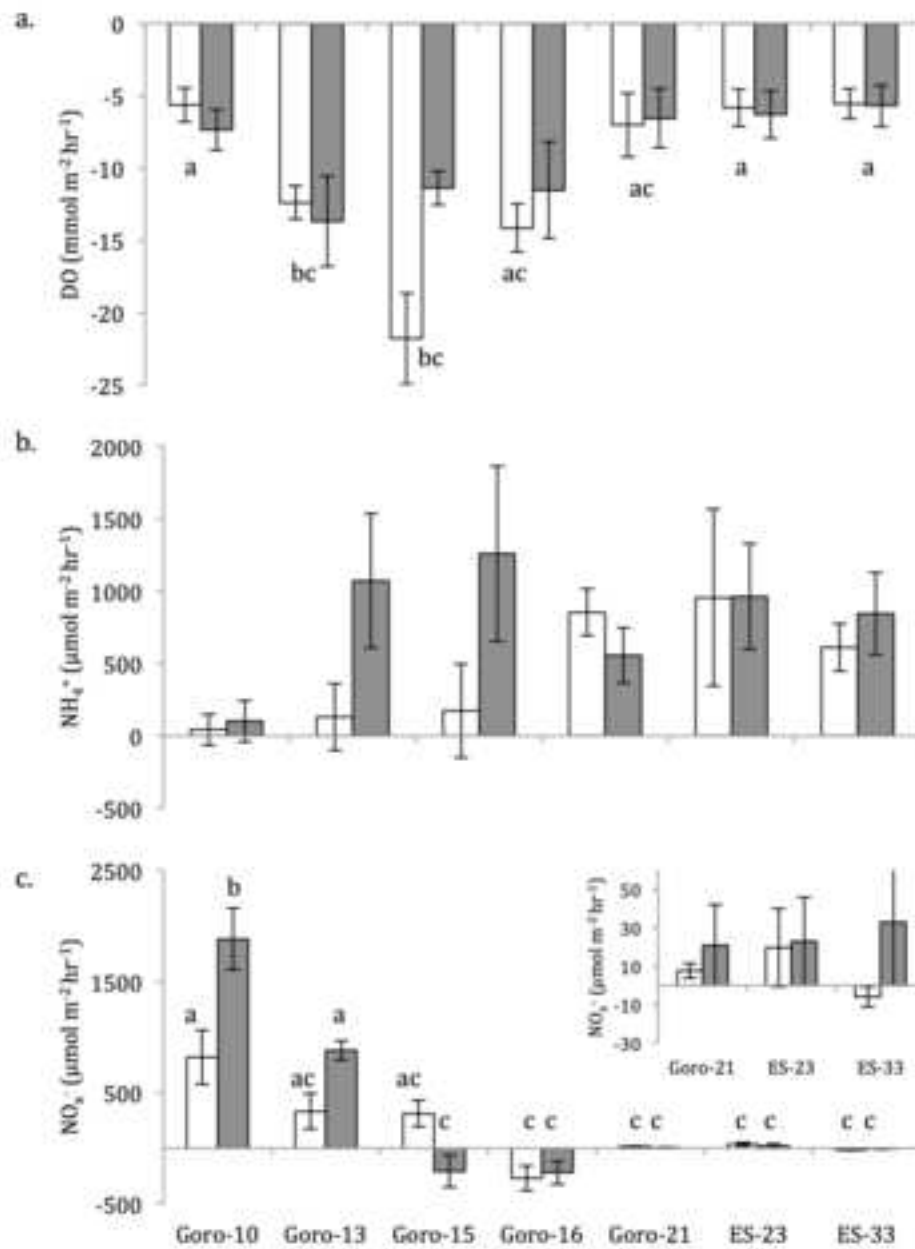


Figure 3
[Click here to download high resolution image](#)

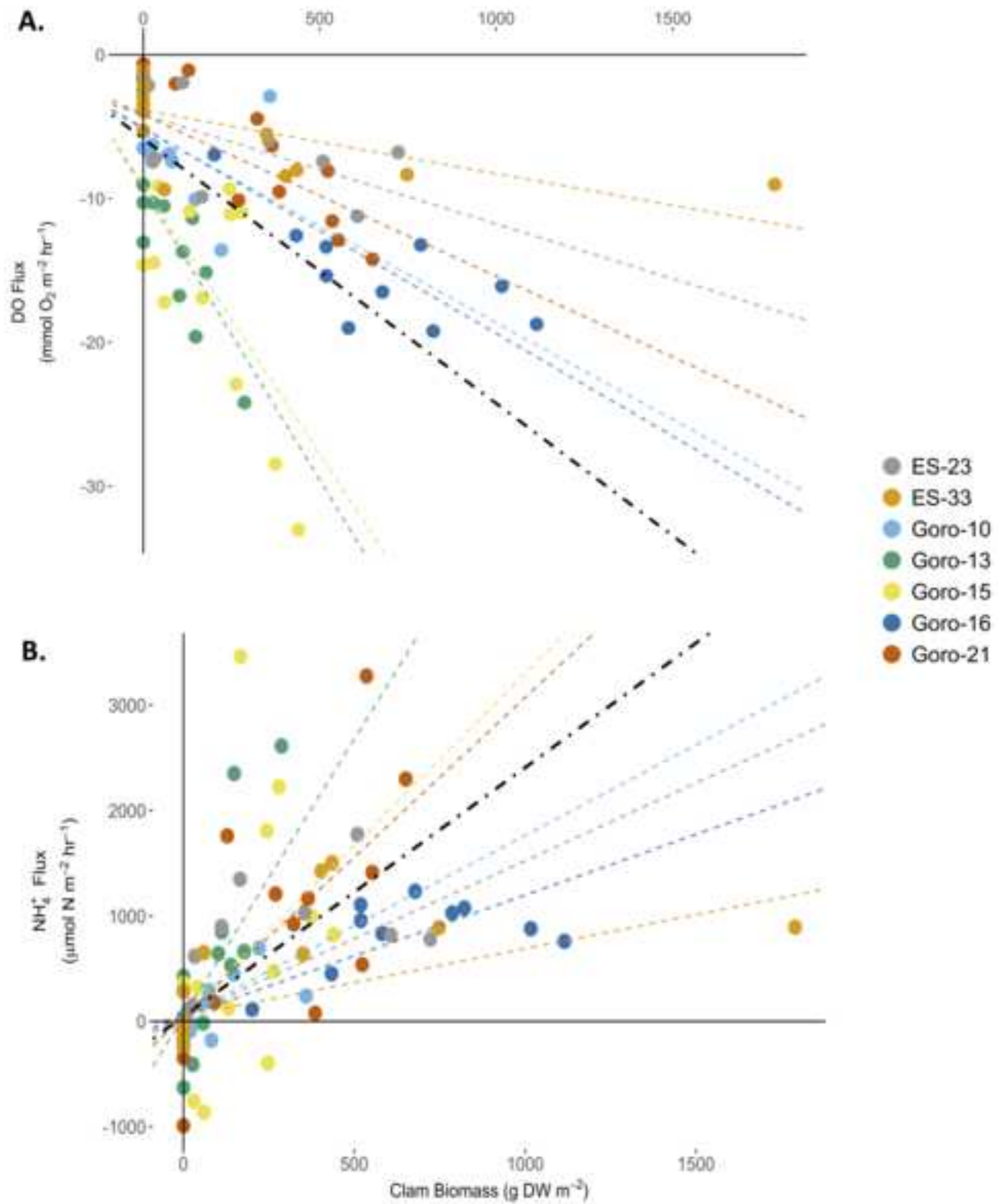


Figure 4

[Click here to download high resolution image](#)

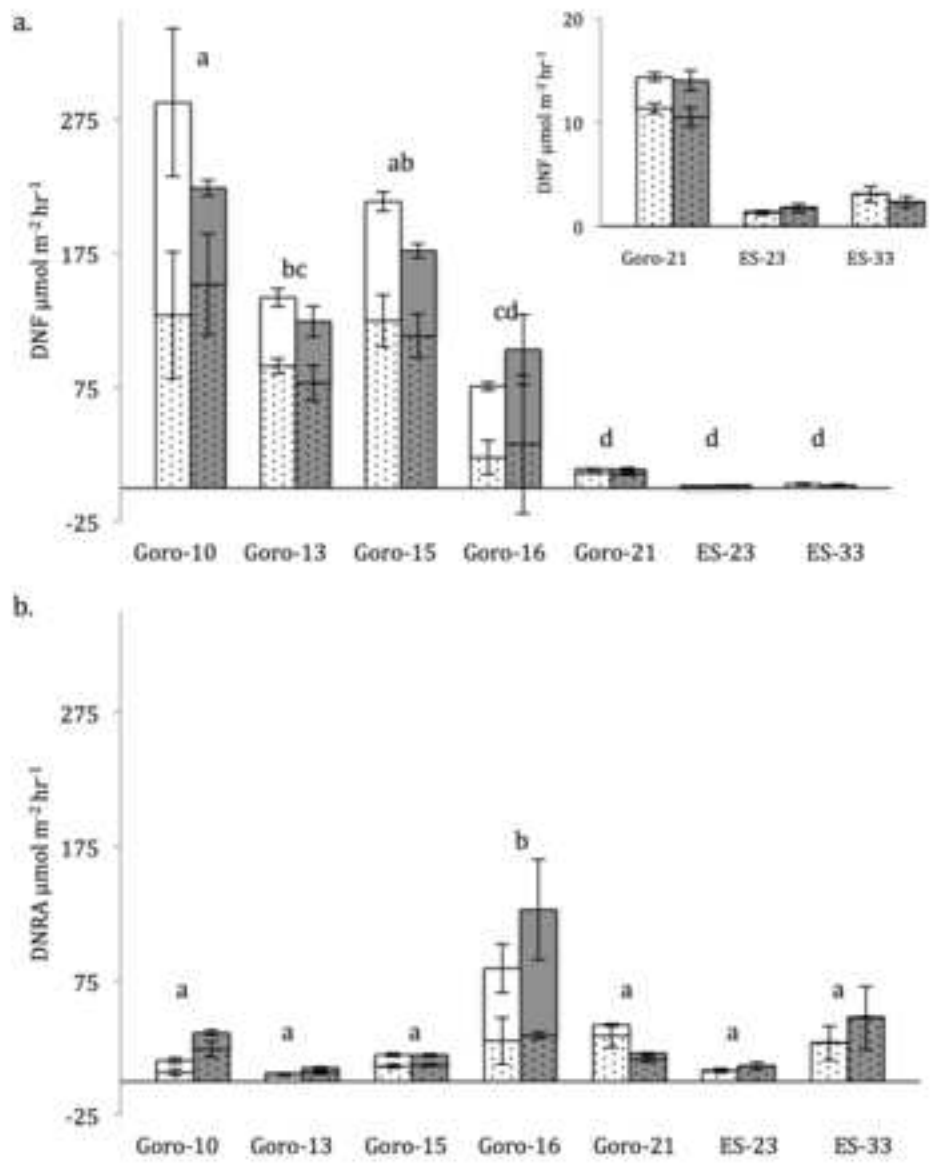


Figure 5

[Click here to download high resolution image](#)

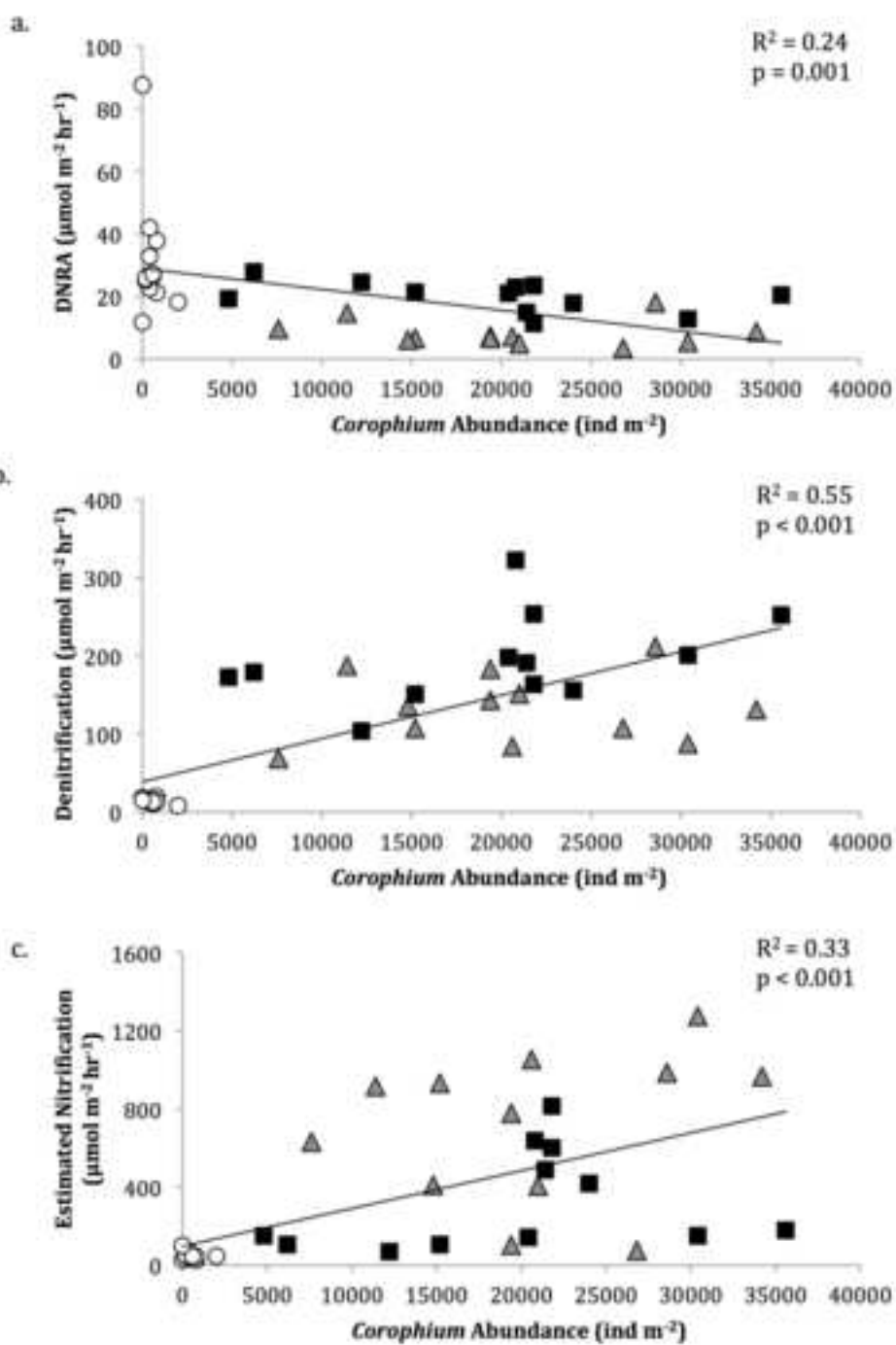


Figure 6
[Click here to download high resolution image](#)

